

A Cloud Nucleus Counter with Long Available Growth Time

A. M. SINNARWALLA AND D. J. ALOFS

*Dept. of Mechanical and Aerospace Engineering and Graduate Center for Cloud Physics Research,
University of Missouri-Rolla*

(Manuscript received 29 November 1972, in revised form 12 February 1973)

ABSTRACT

A vertical plate, steady-flow, thermal diffusion chamber designed for use as a cloud condensation nucleus counter is described. In this instrument, phoretic forces are shown to limit the maximum available growth time to a value eight times larger than the growth time available in conventional horizontal plate chambers. This additional growth time is shown to be necessary when operating at supersaturations below 0.2%. Experiments and calculations concerning convection currents in the vertical chamber are also presented.

1. Introduction

Cloud condensation nuclei (CCN) are commonly counted using horizontal plate, thermal gradient diffusion chambers. A short coming of these chambers is that the small height (usually ~ 1 cm) of the chambers allows the falling water drops to experience a uniform supersaturation for only a short time. To avoid this difficulty a steady-flow vertical diffusion chamber was developed. In this vertical chamber, the available growth time is limited by thermophoretic and diffusiphoretic forces rather than by gravity forces. The first purpose of this paper is to calculate the available growth times in the horizontal and in the vertical chambers, and compare them with the growth times needed to count a reasonably large percentage of the activated CCN. The second purpose is to present experiments and calculations concerning the effects of convection currents in the vertical chamber.

2. Description of the vertical chamber

The chamber features steady, laminar flow of the sample downward between two vertical plates each 100 cm long by 13.2 cm wide, with a plate spacing d of 1 cm (Fig. 1). One plate is kept at a temperature T_h , the hot plate temperature, the other at temperature T_c , the cold plate temperature. For the entire length of the cold plate, and for the lower 85 cm length of the hot plate, the inside plate surfaces are covered with filter paper which is continually supplied with water. The upper 15 cm length of the hot plate, however, is dry to avoid the transient supersaturations described by Fitzgerald (1970) and by Saxena *et al.* (1970).

The sample enters the chamber at temperature T_{in} , and relative humidity ϕ , where T_{in} is always less than T_h . As the sample flows through the chamber, the local temperature T and water vapor pressure p even-

tually become linearly proportional to the distance from the cold plate. This produces the same approximately parabolic supersaturation profile which occurs in the conventional static, or zero flow, thermal diffusion chamber. This parabolic profile is given by Saxena *et al.* (1970), among others. Thus, the supersaturation is a maximum approximately midway between the plates, and drops off rapidly on approach to either plate.

To count the water drops produced, an automatic drop detecting device is being developed for the chamber. Those nuclei which have been condensed upon form water drops which scatter light as they fall one by one through a laser beam (Fig. 1). The scattered light is sensed by a photomultiplier, which in turn activates an electronic counter. This counting device is similar to the optical counters manufactured by Royco, Climet, Southern Research Institute, etc., but has the advantage of counting the drops *in situ*.

3. Magnitude of the phoretic velocities

The diffusiphoretic velocity (V_D , cm sec⁻¹) of sub-micron aerosol particles in an air-water vapor mixture was determined experimentally by Goldsmith *et al.* (1963) to be

$$V_D = -1.9 \times 10^{-4} \frac{dp}{dy}, \quad (1)$$

where dp/dy is the water vapor pressure gradient (mb cm⁻¹).

The thermophoretic velocity (V_T , cm sec⁻¹) of similar particles in air was experimentally found by Goldsmith and May (1966) to be

$$V_T = -2.6 \times 10^{-4} \frac{dT}{dy}, \quad (2)$$

where dT/dy is the temperature gradient ($^{\circ}\text{C cm}^{-1}$).

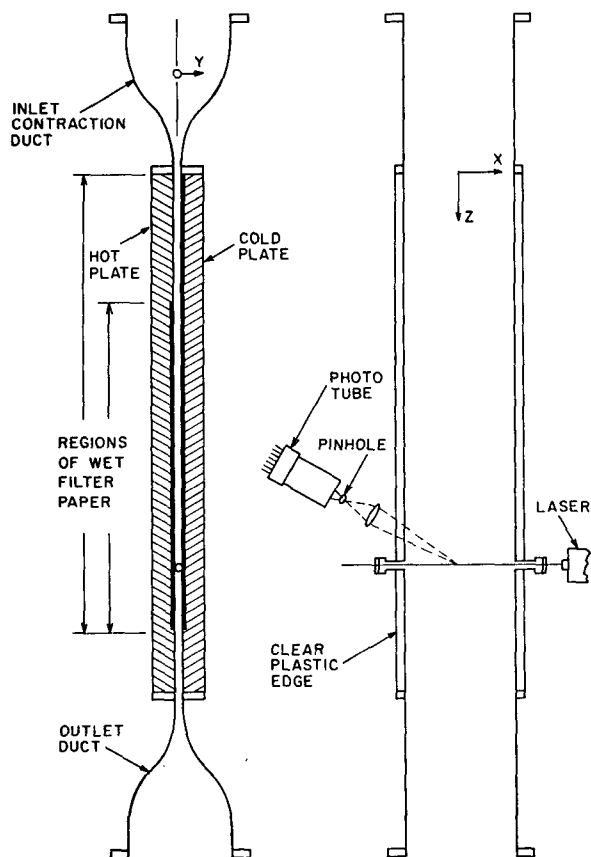


FIG. 1. Schematic of the vertical plate, steady-flow, thermal diffusion chamber.

Consulting vapor pressure data for water, and using $T_h = 25^\circ\text{C}$, and 1-cm plate spacing, (1) can be transformed to the approximate relationship

$$V_D \approx -3.2 \times 10^{-4} \frac{dT}{dy}. \quad (3)$$

Comparing (2) and (3), it can be seen that for sub-micron particles V_D and V_T are approximately equal in the thermal diffusion chamber.

Goldsmith and May (1966) have shown that V_D and V_T are additive, so that the combined phoretic velocity (V_P , cm sec^{-1}) for submicron particles is obtained by adding (2) and (3), i.e.,

$$V_P = -5.8 \times 10^{-4} \frac{dT}{dy}. \quad (4)$$

Eq. (4) is for particles near $0.09 \mu\text{m}$ radius. We now try to estimate how V_D and V_T depend on particle radius r . The critical parameter is the inverse Knudsen number, defined as r/λ , where λ is the molecular mean free path in the gas. For air at 25°C and 1 atm, λ has a value near $0.067 \mu\text{m}$.

Concerning the thermophoretic velocity, experiments by Schadt and Cadle (1961) with various particles in air give a value of V_T at $r/\lambda = 20$ one-third of that at $r/\lambda \ll 1$. This agrees qualitatively with the theory by Brock (1962).

Concerning the diffusiophoretic velocity, there is disagreement. Experiments by Schmitt (1961) in an air-water vapor mixture indicate that V_D is insensitive to particle size for r/λ between 1 and 6, but later experiments by Storozhilova (1964) indicate that V_D at $r/\lambda = 6$ is twice that at $r/\lambda = 1$.

All in all, the above considerations indicate that the combined phoretic velocity cannot be much different than the value given by (4). At $r/\lambda = 6$, Schmitt's data imply a V_P 30% lower than (4), while Storozhilova's data indicate a value 25% higher. For simplicity (4) will be used for any size particle.

The phoretic velocity can also be expressed in terms of S , the percent supersaturation midway between the plates. For $T_h = 25^\circ\text{C}$, the authors have found the following approximate relation to be valid for $S < 5\%$:

$$S = (T_h - T_c)^2 / 25. \quad (5)$$

A similar relation has recently been published by Hudson and Squires (1973).

Now (4) and (5) are combined to give

$$V_P = 2.9 \times 10^{-3} S^{1/2}. \quad (6)$$

4. Available growth time in the vertical chamber

The phoretic forces move all the nuclei and water drops toward the cold plate with a velocity given by (6). Since the supersaturation drops off rapidly on approach to the chamber walls, the phoretic displacement must not be allowed to become too large, or the nuclei will have spent a large fraction of their available growth time in regions having supersaturations much lower than S . Judgment must now be exercised in determining how large a phoretic displacement is allowable. We choose to be conservative, and limit the phoretic displacement to 0.1 cm, which assures that all of the growth time is spent in regions having supersaturations $\geq 0.9S$. Thus, the maximum allowable residence time (t_P , sec) is $(0.1 \text{ cm})/V_P$, or from (6),

$$t_P = 35S^{-1/2}. \quad (7)$$

The maximum available growth time (t_A , sec) equals t_P minus the time required for the supersaturation to rise to its full value (t_R). One of the authors has taken part in deriving an expression for t_R , by first deriving expressions for the temperature and vapor distributions in the various regions of the chamber. These derivations are too lengthy to present here and will be given in a separate paper. However, t_R turns out to be always less than 6 sec, which is small compared to t_P . Thus, in view of the uncertainty in determining the

phoretic velocity, the difference between t_P and t_A will be neglected.

5. Available growth time in the horizontal chamber

Twomey (1967) has analyzed the influence of gravity in the horizontal diffusion chamber. The available growth time is limited by the allowable vertical fall distance, which he takes to be 0.25 cm. The following growth law is used by Twomey :

$$r \frac{dr}{dt} = \beta S. \tag{8}$$

Here r is the particle radius, t time, S the percent supersaturation, and $\beta = 1.2 \times 10^{-8} \text{ cm}^2 \text{ sec}^{-1}$. The fall velocity (U) of a droplet is given by Stokes law

$$U = Kr^2, \tag{9}$$

with $K = 1.2 \times 10^6 \text{ cm}^{-1} \text{ sec}^{-1}$.

Twomey uses (8) and (9) to determine how large the drops are when they fall 0.25 cm. If one uses (8) and (9) to calculate the available growth time for a 0.25-cm fall distance, one obtains

$$t_A = 4.16S^{\frac{1}{2}}, \tag{10}$$

where for simplicity, the supersaturation is treated as constant.

The influence of the phoretic velocity in the horizontal chamber can now be estimated. If we multiply V_P [from (6)] by t_A [from (10)], the maximum phoretic displacement in the horizontal chamber is found to be $1.2 \times 10^{-2} \text{ cm}$, which is insignificant compared to the gravity displacement.

6. Growth time needed to count 80% of the activated nuclei

Saxena and Carstens (1971) have analyzed the growth rates of NaCl and MgCl₂ salt nuclei. Assuming a typical aerosol size distribution, of a linear log (radius)-number form, they calculate the times required for 80% of the activated nuclei to reach visible size, which is taken as 1 μm radius. Their results are shown by curve 3 in Fig. 2 as a function of the applied supersaturation. In order to count more than 80% of the activated nuclei, longer growth times are needed. Likewise, to count a smaller fraction, shorter growth times are sufficient.

It should be noted that curve 3 in Fig. 2 ends at $S = 0.12\%$. This is because nuclei with critical supersaturations below 0.12% are already larger than 1 μm radius when at 100% relative humidity. Thus, when operating a CCN counter at less than 0.12% supersaturation, the lower cut-off size for counting activated nuclei must be larger than 1 μm radius.

Fig. 2 also shows the maximum available growth times for the vertical chamber, curve 1, and for the

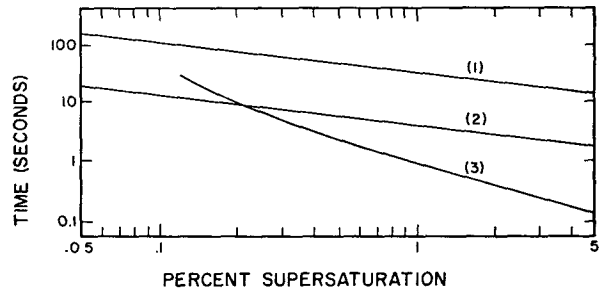


FIG. 2. Growth time vs applied supersaturation. Curve 1: available growth time for the vertical chamber [from Eq. (7)]; curve 2: available growth time for the horizontal chamber [from Eq. (10)]; curve 3: growth time needed to count 80% of the active nuclei (from Saxena and Carstens, 1971).

horizontal chamber, curve 2. These come from (7) and (10), respectively.

One can now make the following conclusions from Fig. 2. First, the horizontal chamber will count fewer than 80% of the activated nuclei when $S < 0.2\%$. Second, the vertical chamber can be used at much lower supersaturations than can the horizontal. Finally, for typical nuclei distributions, the two counters should disagree by at most 20% at $S = 0.2\%$, and at higher S , they will disagree by even less.

7. Convection currents: Theory

Because of the vertical orientation of the plates, there is an upward buoyancy force near the hot plate, and a tendency for backflow there. Bird *et al.* (1960) present a solution of the flow between two infinite vertical parallel plates of different temperature. In their analysis they focus attention on the case of zero net vertical mass flux, but their equation 9.9-12 clearly includes the case of a forced convection superimposed upon the free convection, and indicates that the resulting velocity profile is given by superposition. From their solution, the local fluid velocity V is given as

$$V = [1 - (2y/d)^2][V_c + C(2y/d)], \tag{11}$$

where V is positive downward and negative upward, y is the Cartesian coordinate shown in Fig. 1, d the distance between the plates, and V_c the centerline velocity, that is, V at $y = 0$. The quantity C is defined as

$$C = \rho\beta g d^2 (T_h - T_c) / (48 \mu), \tag{12}$$

where ρ is the average fluid density, β the coefficient of thermal volume expansion, g the gravitational acceleration, and μ the fluid viscosity.

The velocity profiles given by (11) are plotted in Fig. 3 for $T_h = 25\text{C}$, $T_c = 20\text{C}$, and various values of V_c [cm sec⁻¹]. It can be seen that for sufficiently small values of V_c , a backflow develops near the hot plate. This backflow is undesirable for reasons described in Section 9 of this paper. To avoid the backflow, V_c is therefore always kept larger than the following value,

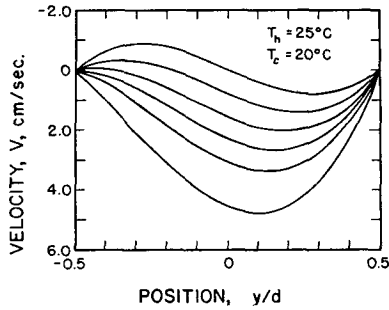


FIG. 3. Velocity profiles obtained from Eq. (11) for $T_h = 25^\circ\text{C}$, $T_c = 20^\circ\text{C}$.

obtained from a suitable evaluation of (11):

$$V_c = 0.43(T_h - T_c). \tag{13}$$

8. Convection currents : Experiments

The solution given in (11) is for infinite parallel plates, and thus does not apply near the front and back edges of the chamber, nor near the entrance and exit regions. One would expect that on approach toward the front or back edge of the chamber, the velocity there merely attenuates to zero, without serious consequences. Concerning the velocity field in the entrance and exit regions of the chamber, the following experiments were performed.

First consider the convective circulation which occurs when the inlet and outlet ducts are blocked off. Experiments in an early version of the chamber, using a smoke visualization technique, indicate that the flow is then as shown on the left side of Fig. 4. For the dimensions of this early chamber, which is 61 cm high by 13 cm wide, with a 1 cm plate spacing, the crossover regions are at most 8 cm high, and in the rest of the chamber (the middle region) the flow is only vertical. It should be mentioned that the smoke visualization technique involved introducing discrete puffs of smoke into the chamber, then closing the chamber and observing the movement of the smoke puffs.

When a downward flow is superimposed upon the free convective flow, one expects streamlines as shown on the right side of Fig. 4. We now use (11) to estimate the expected magnitude of the horizontal deflections experienced in the crossover regions.

The volume flow rate (Q , $\text{cm}^3 \text{ sec}$) of the convective circulation can be obtained by integrating (11) between the limits $y=0$ and $y=d/2$ for the case $V_c=0$. This gives

$$Q = 0.054b(T_h - T_c), \tag{14}$$

where b is the plate width (cm). Thus, the horizontal velocity (H , cm sec^{-1}) in the crossover regions is approximately

$$H = 0.054(T_h - T_c)/L, \tag{15}$$

where L is the vertical length (cm) of the crossover regions.

The residence time near $y=0$ in the crossover regions is L/V_c . Thus, the horizontal deflection is HL/V_c , which from (13) and (15) turns out to have a maximum value of 1.3 mm.

An attempt was then made to verify this result experimentally. A thin line of smoke was injected continuously midway between the plates, as depicted on the right side of Fig. 4. With the sample velocities given by (13), the smoke line was found to be a slanted straight line, with the smoke moving 1 mm toward the cold plate over a 60 cm length of the chamber. Such behavior is due to phoretic displacement, and is in accord with (6). However, the horizontal deflection back toward the hot plate, which one expects in the lower crossover region, was not observed. If such a deflection was present, it was less than 0.5 mm, which we estimate to be the accuracy of the visualization technique. We infer that either (14) overestimates the convective circulation, or else the crossover occurs in the inlet contraction duct and outlet expansion duct.

9. Convection currents : Discussion

Saxena and Carstens (1971) analyze convection effects in a thermal diffusion chamber having cylindrical vertical walls. The downward flow velocity for that chamber is much smaller than the average convection velocity, and therefore many of the nuclei experience several passes up the hot wall, and down the cold wall. Saxena and Carstens also consider what happens as a parcel of air passes through the crossover regions, where the air is assumed to pass completely from one

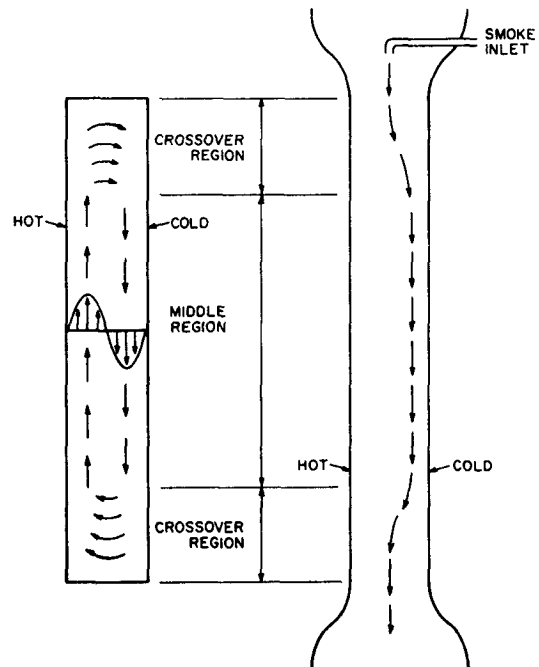


FIG. 4. Depiction of smoke experiments.

wall to the other wall. They find a transient supersaturation at the lower crossover region, and show that it probably influences the nuclei count.

Obviously the characteristics of the present chamber differ significantly from those of the chamber analyzed by Saxena and Carstens. The horizontal deflections experienced by parcels of air in the present chamber are less than one-tenth of the distance between the plates, so transient supersaturations would be much smaller than the values they predict. Moreover, any transient supersaturation in the lower crossover region, which is the only place one can occur, could not influence the nuclei count, because the lower crossover region is downstream of the region where the nuclei are counted. Since there is no upward flow in the chamber, a nucleus in the lower crossover region is never recirculated. It therefore seems that convection currents could not influence the nucleus count in the present chamber.

10. Nuclei counts

Fig. 5 shows nuclei counts taken with room air stored in a 575-liter plastic bag. The relative humidity in the bag was 50%, and the plate temperatures were $T_h = 26^\circ\text{C}$, $T_c = 23^\circ\text{C}$, giving an operating supersaturation of 0.36%. It should also be noted that the water drops were counted at $z = 50$ cm (Fig. 1) which is 35 cm downstream of the position where the filter paper begins on the hot plate.

The ordinate in Fig. 5 is the nuclei count, taken photographically in this case, and the upper scale on the abscissa is the sample velocity midway between the plates. The lower scales on the abscissa show the available growth time and the phoretic displacement.

One obvious feature exhibited by the data is that as the available growth time is increased from 3.5 to 20 sec, the nuclei count increases. This is in accord with curve 3 of Fig. 2, which predicts a 3.8-sec required growth time to count 80% of the active nuclei. Data obtained at 1% supersaturation exhibit an almost constant nuclei count for this same range of available growth time, and this is also in accord with curve 3 of Fig. 2.

Fig. 5 shows a decrease in the count as the flow rate is decreased below 1.3 cm sec $^{-1}$, where the backflow begins. As discussed above, the chamber should not be operated in this regime.

11. Conclusions

A vertical diffusion chamber has been built and appears to be operating in accord with theoretical calculations. Phoretic forces limit the available growth time in the new chamber. Nevertheless, the available growth time is larger by a factor of 8 than that in the

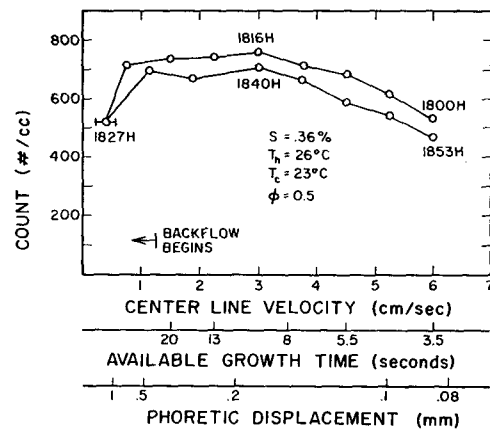


FIG. 5. Nuclei counts obtained with the vertical chamber using room air.

horizontal chamber. This additional growth time is necessary when operating at supersaturations $< 0.2\%$.

Acknowledgments. The stimulus and enjoyment of many conversations with Drs. J. L. Kassner, Jr., J. C. Carstens and J. F. Stampfer, Jr., is acknowledged with gratitude. This work was supported by the National Science Foundation under Grant GA-30876 of the Atmospheric Sciences Section.

REFERENCES

- Bird, R. B., W. E. Stewart and E. N. Lightfoot, 1960: *Transport Phenomena*. New York, Wiley, 298-300.
- Brock, J. R., 1962: On the theory of thermal forces acting on aerosol particles. *J. Colloid. Sci.*, **17**, 768-780.
- Fitzgerald, J. W., 1970: Non-steady-state supersaturations in thermal diffusion chambers. *J. Atmos. Sci.*, **27**, 70-72.
- Goldsmith, P., and F. G. May, 1966: Diffusiophoresis and thermophoresis in water vapour systems. *Aerosol Science*, C. N. Davis, Ed., New York, Academic Press, 163-194.
- , H. J. Delafield and L. C. Cox, 1963: The role of diffusiophoresis in the scavenging of radioactive particles from the atmosphere. *Quart. J. Roy. Meteor. Soc.*, **89**, 43-61.
- Hudson, J., and P. Squires, 1973: Evaluation of a recording continuous cloud nucleus counter. *J. Appl. Meteor.*, **12**, 175-183.
- Saxena, V. K., and J. C. Carstens, 1971: On the operation of cylindrical thermal diffusion chambers. *J. Rech. Atmos.*, **5**, 11-23.
- , J. N. Burford and J. L. Kassner, Jr., 1970: Operation of a thermal diffusion chamber for measurements on cloud condensation nuclei. *J. Atmos. Sci.*, **27**, 73-80.
- Schadt, C. F., and R. D. Cadle, 1961: Thermal forces on aerosol particles. *J. Phys. Chem.*, **65**, 1689-1694.
- Schmitt, K. H., 1961: Untersuchungen und Schwebstoffteilchen in diffundierendem Wasserdampf. *Z. Naturforsch.*, **16a**, 144-149.
- Storozhilova, A. I., 1964: Measurement of the velocity of aerosol particles in a steam diffusion field. *Dokl. Akad. Nauk. SSSR*, **155**, 426-429.
- Twomey, S., 1967: Remarks on the photographic counting of cloud nuclei. *J. Rech. Atmos.*, **3**, 85-90.